Physical and mechanical properties of interface transition zone between loess and paleosol

Xianglin Peng[1,*], Wen Fan[1], Chao Sun[2], Guang Hao[3], Ying Zhang[4]

1. Chang'an University, Xi'an 710054, China.

2. Shaanxi Nuclear Industry Engineering Survey Institute Company Limited, Xi'an 710000, China

3. Prospecting Branch Institute, Yunnan Design Institute Group, Kunmin 650228, China

4. Geological Exploration and Research Institute of LNYS, Liaoning 110013, China

   195259645@qq.com

ABSTRACT. This paper explores the physical and mechanical properties of interface transition zone between loess and paleosol. Four samples were collected from Jingyang in the southeast of the Chinese Loess Plateau, and subjected to site and lab shear tests, aiming to disclose the shear behavior of interface transition zone, which contains landslide hazards. The results show that the strength parameters of loess decreased by nearly 2/3 (a 18.8kPa drop in C value and an 8.7° decrease in φ value), and the interfacial transition zone and paleosol decreased by less than 10% from the natural state to the saturated state. This means the interfacial transition zone is a natural slip bed of landslide.

RÉSUMÉ. Cet article explore les propriétés physiques et mécaniques de la zone de transition d'interface entre le lœss et le paléosol. Quatre échantillons ont été recueillis à Jingyang, au plateau de Loess au sud-est de la Chine, et soumis à des tests de cisaillement sur place et en laboratoire, dans le but de révéler le comportement de cisaillement de la zone de transition d'interface, qui présente des risques de glissement de terrain. Les résultats montrent que les paramètres de résistance du lœss ont diminué de près de 2/3 (diminution de 18,8 kPa de la valeur C et de 8,7 ° de la valeur φ), ainsi que la diminution de moins de 10% de la zone de transition d'interface et du paléosol entre l'état naturel et l'état saturé. Cela signifie que la zone de transition d'interface est un siège naturel de glissement de terrain.

KEYWORDS: interface transition zone, loess paleosol, large shear test, shear characteristics.

MOTS-CLÉS: zone de transition d'interface, lœss et paléosol, test de grand cisaillement, caractéristiques de cisaillement.
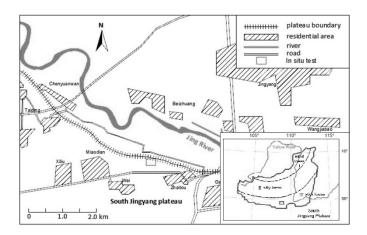
1. Introduction

The loess-paleosol interface transition zone is the zone between loess and paleosol. Previous studies have shown that the interfacial transition zone of the two materials is the region where the material properties change, and is usually the weaker region between the materials. This difference in properties tends to cause damage to the material.

Both loess and paleosol are soil materials formed by Quaternary aeolians, with the difference being the difference in climate and subtle composition during formation. Since the sediment thickness of loess is much larger than that of paleosol, it is often overlooked in the study of paleosol (Chen *et al.*, 1997).

At present, there are many research results on loess, including agriculture, paleoclimate, age, physical mechanics and so on. Research on paleosol is less and mainly concentrated on age and causes (Lu and An, 1998; Wang *et al.*, 2014), until some scholars (Deng *et al.*, 2015) have noticed that certain properties of paleosol can cause some geological disasters, such as landslides and collapses. But the material properties of the loess-paleosoil interface transition zone has not yet been found to have any research results (Fan *et al.*, 2017; Huang *et al.*, 2008).

The aim of this research is to study the physical and mechanical properties of the loess-paleosol interfacial transition zone (abbreviated as ITZ). Based on this, a supplementary discussion of some research mechanisms proposed by scholars is made (Lei and Wei, 1998; Sprafke & Obreht, 2016).

2. Samples and method

Figure 1. Location of study area

The test site and the samples studied were obtained from the south Jingyang

platform on the south margin of the Chinese Loess Plateau. The loess and paleosol from top to bottom in order of formation are named L_x and S_x, respectively, where x is the layer number. There are a large number of landslides on site, and in order to ensure sample integrity and less perturbation, samples are taken 2 meters inward of the landslide wall. The selected formation is L_2, the interface transition zone and S_2.
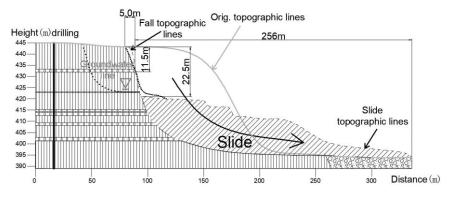

Figure 2. Stratum profile and typical disasters

The physical properties of the five samples were measured according to the Chinese standard method for soil testing (GB/T 50123-2008). Samples were dried for 12 hours at temperature of 105 °C to determine the moisture content. The density was tested through cutting an undisturbed sample using a standard cutting ring with diameter of 61.8 mm and height of 20 mm. The liquid limits and plastic limits were determined by means of a cone penetrometer. The mineral compositions were analyzed using X-ray powder diffraction (XRD). The particle size distributions were measured using a laser particle analyzer. The penetration was tested through triaxial test with a standard sample having a diameter of 39.1 mm and a height of 80 mm. The mechanical behavior of loess and paleosol was studied by laboratory direct shear test (GB/T 50123-2008), the mechanical properties of the loess-paleosol interface transition zone were studied by in site experiments (Xiao *et al.*, 1995; Xu *et al.*, 2012; Zhang *et al.*, 2013).

Table 1. General physical parameters

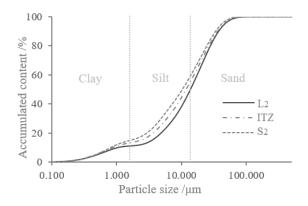| Types	Depth /m	Nature moisture content /%	Density/ g•cm³	Pore ratio e	Liquid limit /%	Plastic limit /%
L_2	21.8	16.6 ±0.47	1.67 ±0.03	0.888	33.72 ±0.37	16.82 ±0.30
ITZ	22.0	24.8 ±0.20	1.80 ±0.02	0.872	30.01 ±0.22	20.95 ±0.35
S_2	22.2	21.3 ±0.38	1.86 ±0.03	0.775	28.70 ±0.34	19.77 ±0.42

Figure 3. Grading curve

Table 2. Main mineral component

Mineral composition	Quartz	Plagioclase	Potash feldspar	Clay minerals	Calcite	Amphibole
L2	57.0%	14.5%	2.0%	11.0%	15.0%	0.5%
ITZ	63.0%	11.5%	5.0%	12.0%	8.0%	0.5%
S2	71.0%	9.0%	1.0%	13.0%	6.0%	0.0%

Table 3. Permeability coefficient k/10-9m/s

Surrounding pressure/kPa		50	100	200	300	400	500
L_2	Horizontal	320	205	76	43	30	24
	Vertical	620	425	173	90	57	46
ITZ	Horizontal	234	158	63	34	23	20
	Vertical	470	323	137	72	45	37
S_2	Horizontal	148	110	49	24	16	15
	Vertical	320	220	101	54	32	27

ITZ's soil height is limited, and the shear test in the laboratory will be more disturbing, so the in-situ test is a better choice. According to location of ITZ, dig 250mm downwards as the base surface, make an in-situ block of a side length of 700mm square, and make both sides of the sample parallel to the wall. Further refinement of the block of 495±2mm on the side and then it is inserted into the shear box. The upper and lower shear boxes have wooden clips with a diameter of 2mm.

The gap between the specimen and the shear box was filled with fine sand for 10 times and shocked with a steel rule. With the shear box as the center, an annular groove with a diameter of 800 mm, a width of 10 mm, and a depth of 100 mm was cut on the base surface. A plastic film is pressed in it and then it is set into a saturator. A compacted soil with a height of 100 mm is filled at the bottom of the saturator to assist the seal. Fill the saturated appliances with water until flooding the top of the sample. Place a 100L bucket next to the sample, maintain a flow rate of 5L / h through the valve, and replenish the water every 12 hours.
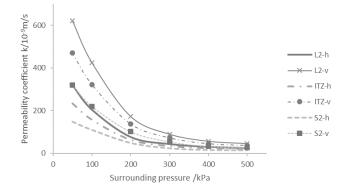

Figure 4. Permeability coefficient k curve

Table 4. laboratory shear result

State		L2	S2
nature	c	30.5	48.5
	φ	19.6	29.2
saturated	c	11.7	44.6
	φ	10.9	28.6

Table 5. The test scheme

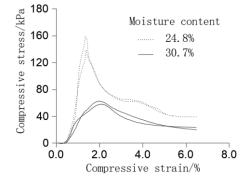| Moisture content	Maximum load (kPa)	Design load (kPa)		
Natural (24.8%)	158	90	120	150
Saturated (30.7%)	61	30	40	50

Figure 5. The unconfined uniaxial compressive strength

The maximum vertical load was obtained by an unconfined uniaxial compression test. The results are shown in Figure 4. The final load scheme is shown in Table 5. A graded method is adopted in the vertical loading method. In order to ensure that the sample will not be destroyed due to a single load, the single-stage load is controlled to 5 kN. When the vertical deformation rate is less than 0.05 mm/h, the deformation is stable and the next-level load is loaded. The horizontal load begins after the stabilization of final load deformation. The horizontal loading also adopts the method of graded loading and the single-stage loads load is controlled to 5 kN. When the deformation rate is less than 0.05 mm/min or it maintains a constant speed for 10 min, it is loaded into the next level. When the shear stress is not maintained at a certain level for long time, or even decreases, or the deformation amount reaches 10%, it is considered that the sample has been destroyed.

3. Results

3.1. Physical properties

Table 1 shows that the liquid limit of the samples was in range of 28.70–33.72 %, the plastic limit was 16.82–20.95 %, the pore ratio was 0.775–20.888, and the moisture content was 16.6-21.3%. The physical index indicates that the loess is larger than the interfacial transition zone and the paleosol is the smallest. However, the interfacial transition zone is the highest in the moisture content, followed by the paleosol and the loess.

Table 2 shows that the samples mainly contained quartz (57.0–71.0%), feldspar (10.0–16.5%), calcium (6.0–15.0%) and clay minerals (11.0–13.0%). Loess samples generally had higher calcium and feldspar contents, but lower clay mineral and quartz contents than paleosol samples, the interface transition zone was in the middle.

Table 3 shows the variation of the permeability coefficient of the sample. The

vertical permeability coefficient is greater than the horizontal permeability coefficient, and the loess is larger than the interface transition zone than the paleosol.

Figure 3 shows that the particle size of the samples was generally less than 75 μm and the main part was silt (2-20 μm). The clay (less 2μm) fraction of the sample (less than 2 μm) was 11-19%.

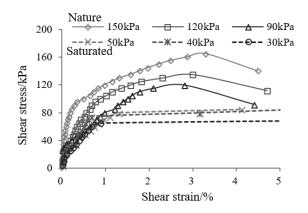### 3.2. In site shear experiments of ITZ

Figure 6. ITZ shear stress-strain curve of in-situ test
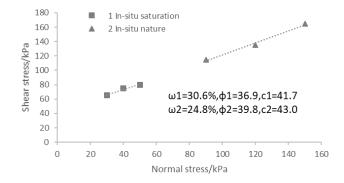

Figure 7. Shear strength envelope of in-situ and laboratory

According to the test results, the stress-strain curves in saturated and natural state are drawn, as shown in Figure 6. In saturated conditions, the sample curve is strain-hardened and the stress increases linearly with strain. The shear strain peaks at around 1%, and the strain increases continuously. However, the stress does not

increase. Under natural conditions, the sample curve is strain-softening. The shear strain reaches its peak at 3%, and the soil stress decreases with the increase in strain. Under natural and saturated conditions, the strain corresponding to the peak strength of the sample increases with normal stress.

According to the Coulomb formula, the shear strength parameters at different moisture content were obtained, it is shown in Figure 7.

Table 6. Shear fluctuation characteristics

Nature	Max undulation	Saturated	Max undulation
150kPa	6mm	50	
120kPa	15mm	40	Muddy state, straight and smooth.
90kPa	24mm	30	

3.3. Shear fluctuation characteristics of ITZ

Under the natural moisture content, the maximum undulation height of the 150 kPa shear plane is about 6 mm, and a large area of relatively smooth and fine scratches appears along the shear direction; the maximum undulation height of the 120 kPa shear plane is about 15 mm, and the undulation is mainly concentrated in the middle, along the In the direction of shearing, the scratches at the beginning are relatively smooth, and there are small flaky scratches in the middle, and many small cracks in the middle; the 90 kPa shear surface has a large undulation, the maximum undulation height is about 24 mm, the scratch is rough and not smooth, and more loose. The particles and the fine cracks are irregularly extended in the direction of extension. Under saturated conditions, the sheared surface is muddy and the sheared surface is straight and smooth.

4. Discussion

4.1. Permeability coefficient

The permeability coefficient k has a correlation with the particle composition and mineral composition of the soil. Figure 3-4 shows that the clay and silt content are gradually increased in the interfacial transition zone and paleosol. The growth of fine particles will make the pores denser and the permeability coefficient k will decrease. The clay minerals expand when exposed to water, so an increase in the clay mineral content also causes a decrease in the permeability coefficient k.

The decrease of the permeability coefficient of different soil layers will cause local stagnant water inside the bottom soil (Duan *et al.*, 2016), which is also the reason for the high natural moisture content of the interfacial transition zone in

Table 1. It is further assumed that when the accumulated water further increases, localized loess on the interfacial transition zone will be saturated.

4.2. Shear fluctuation characteristics

The essence of shearing is the particle displacement. The particles randomly expand along the direction of the connecting defect under the shear stress, and gradually form micro-cracks, and the micro-cracks are connected to each other to form a shearing surface. When the moisture content is relatively low, the connection ability between soil particles is relatively strong, the displacement ability is weak, and a complete shear plane can be formed after shearing. Under saturated conditions, the soil particles have relatively strong displacement capacity and weak connection ability, which can quickly fill interparticle defects and shear cracks, so the shear surface is relatively flat and smooth.

The undulation of the shear plane is related to the growth of random defects. Under low overburden pressure, the interparticle pressure is small, the range of random defect expansion is relatively large, and the cracking crack is also more; the higher the overburden pressure, the greater the interparticle pressure, and the smaller the range of random defect expansion.

4.3. Strength parameters

Table 4 and Figure 6 show that in the cohesion parameter, the loess is smaller than the interfacial transition zone, and the paleosol is the largest. The internal friction angle, the loess is smaller than the ancient soil, and the interface transition zone is the largest. The strength parameter is affected by the moisture content, the increase in moisture content will cause the strength parameters of the sample to decrease. The impact of ITZ and paleosol is relatively low, the strength parameter decreases less than 10%. The impact of loess is large, the strength parameter decreases about 2/3. Compare with loess, ITZ still has high strength under saturated conditions. as a structure of upper soft and lower hard, it still is a natural slip bed of the landslide.

5. Conclusions

The physical and mechanical properties of loess-paleosol interface transition zone from China, including the moisture content, liquid limits, plastic limits, mineral compositions, particle size, penetration and shear behavior.

The results of the study show that the changes in liquid limits, plastic limits, mineral compositions, particle size, and penetration have obvious regularity, and the value of the interface transition zone is between loess and paleosol. Influenced by particle composition and mineral composition, the interfacial transition zone and the permeability of loess and paleosol have significant differences. The decrease of the

permeability coefficient of different soil layers will cause local stagnant water inside the bottom soil.

The strength parameter is affected by the moisture content, the increase in moisture content will cause the strength parameters of the sample to decrease. The impact of ITZ and paleosol is relatively low, the strength parameter decreases less than 10%. The impact of loess is large, the strength parameter decreases about 2/3. Compare with loess (Wei *et al.*, 2017), ITZ still has high strength under saturated conditions. As a structure of upper soft and lower hard, it still is a natural slip bed of the landslide.

Acknowledgment

References

Chen F. H., Bloemendal J., Wang J. M., Li J. K., Oldfied F. (1997). High-resolution multi-proxy climate records from Chinese Loess: Evidence for rapid climatic changes over the last 75 kyr. *Palaeogeogr Palaeoclimatol Palaeoecol*, Vol. 130, No. 1-4, pp. 323-335. https://doi.org/10.1016/S0031-0182(96)00149-6

Deng J., Zhang Y, Wang J. (2015). Shear strength characteristics of loess paleosol. *Bulletin of Soil & Water Conservation*, Vol. 5, pp. 319-322. https://doi.org/10.13961/j.cnki.stbctb.2015.05.059

Duan Z., Peng J., Leng Y. (2016). Physico-mechanical characteristics of Q2 loess in South Plateau of Jingyang. *Journal of Chang'an University (Natural Science Edition)*, Vol. 36, No. 5, pp. 60-66, 109. https://doi.org/10.19721/j.cnki.1671-8879.2016.05.009

Fan W., Deng L., Yuan W. (2017). Double parameter binary-medium model of fissured loess. *Engineering Geology*, Vol. 31, No. 11, pp. 1752-1756. https://doi.org/10.1016/S1874-8651(10)60073-7

Huang J., Zhang W., Zuo J. (2008). An overview of the semi-arid climate and environment research observatory over the loess plateau. *Advances in Atmospheric Sciences*, Vol. 25, No. 6, pp. 906. https://doi.org/10.1007/s00376-008-0906-7

Lei X., Wei Q. (1998). Study on the origin and countermeasure of the casualty loess landfalls in the Northern Shaanxi. *Chinese Jounal of Geotechnical Engineering*, No. 1, pp. 64-70.

Lu H., An Z. (1998). Paleoclimatic significance of grain size of loess-palaeosol deposit in Chinese Loess Plateau. *Science in China Series D: Earth Sciences*, Vol. 41, No. 6, pp. 626-631.

Sprafke T., Obreht I. (2016). Loess: rock, sediment or soil–what is missing for its definition. *Quaternary International*, Vol. 399, pp. 198-207.

https://doi.org/10.1016/j.quaint.2015.03.033

Wang H., Chen J., Zhang X. (2014). Palaeosol development in the Chinese Loess Plateau as an indicator of the strength of the East Asian summer monsoon: Evidence for a mid-Holocene maximum. *Quaternary International*, Vol. 334, pp. 155-164. https://doi.org/10.1016/j.quaint.2014.03.013

Wei Y., Fan W., Cao Y. (2017). Experimental study on the vertical deformation of aquifer soils under conditions of withdrawing and recharging of groundwater in Tongchuan region, China. *Hydrogeology Journal*, Vol. 25, No. 2, pp. 297-309. https://doi.org/10.1007/s10040-016-1498-4

Xiao J., Porter S. C., An Z. (1995). Grain Size of Quartz as an Indicator of Winter Monsoon Strength on the Loess Plateau of Central China during the Last 130,000 Yr. *Quaternary Research*, Vol. 43, No. 1, pp. 22-29. https://doi.org/10.1006/qres.1995.1003

Xu L., Qia X., Wu C. (2012). Causes of landslide recurrence in a loess platform with respect to hydrological processes. *Natural Hazards*, Vol. 64, No. 2, pp. 1657-1670. https://doi.org/10.1007/s11069-012-0326-y

Zhang M. S., Wei H. U., Zhu L. F. (2013). The method for large scale in-situ shear test of saturated soils and its application. *Geological Bulletin of China*, Vol. 32, No. 6, pp. 919-924. https://doi.org/10.1007/978-3-319-05050-8_28